Comprehensive analysis of the metabolomics and transcriptomics uncovers the dysregulated network and potential biomarkers of Triple Negative Breast Cancer

Sisi Gong[1], Rongfu Huang[1], Meie Wang[1], Fen Lian[1], Qingshui Wang[2*], Zhijun Liao[3*] and Chunmei Fan[1*]

Abstract

Triple-negative breast cancer (TNBC) is known for its aggressive nature, lack of effective diagnostic tools and treatments, and generally poor prognosis. The objective of this study was to investigate metabolic changes in TNBC using metabolomics approaches and explore the underlying mechanisms through integrated analysis with transcriptomics. In this study, serum untargeted metabolic profiles were first examined between 18 TNBC patients and 21 healthy control (HC) subjects using liquid chromatography-mass spectrometry (LC-MS), identifying a total of 22 significantly differential metabolites (DMs). Subsequently, receiver operating characteristic analysis revealed that 7-methylguanine could serve as a potential biomarker for TNBC in both the discovery and validation sets. Additionally, transcriptomic datasets were retrieved from the GEO database to identify differentially expressed genes (DEGs) between TNBC and normal tissues. An integrative analysis of the DMs and DEGs was conducted, uncovering potential molecular mechanisms underlying TNBC. Notably, three pathways—tyrosine metabolism, phenylalanine metabolism, and glycolysis/gluconeogenesis—were enriched, providing insight into the energy metabolism disorders in TNBC. Within these pathways, two DMs (4-hydroxyphenylacetaldehyde and oxaloacetic acid) and six DEGs (MAOA, ADH1B, ADH1C, AOC3, TAT, and PCK1) were identified as key components. In summary, this study highlights metabolic biomarkers that could potentially be used for the diagnosis and screening of TNBC. The comprehensive analysis of metabolomics and transcriptomics data offers a validated and in-depth understanding of TNBC metabolism.

Keywords Triple-negative breast cancer, Metabolomics, Transcriptomics, Biomarker, Pathways

*Correspondence:
Qingshui Wang
wangqingshui@fjnu.edu.cn
Zhijun Liao
liaozj100@163.com
Chunmei Fan
13600718981@163.com
[1]The Clinical Laboratory Center, the Second Affiliated Hospital of Fujian
Medical University, Quanzhou, P.R. China
[2]College of Integrative Medicine, Fujian University of Traditional Chinese
Medicine, Fuzhou, P.R. China
[3]Department of Biochemistry and Molecular Biology, School of Basic
Medical Sciences, Fujian Medical University, Fuzhou, P.R. China

Gong *et al. Journal of Translational Medicine*   (2024) 22:1016

Page 2 of 17

Introduction

The intricate nature of breast cancer (BC), characterized by its diverse subtypes, is particularly highlighted by the clinical challenges associated with Triple Negative Breast Cancer (TNBC). Accounting for an estimated 10–15% of all BC cases, TNBC is distinguished by its aggressive cellular behavior, increased likelihood of recurrence, and generally poorer prognostic outcomes [1, 2]. The hallmark of TNBC is its absence of estrogen and progesterone receptors, in addition to a minimal expression of the human epidermal growth factor receptor 2 (HER2) [3], which significantly diminishes the efficacy of standard hormone therapies and HER2-targeted treatments. This situation underscores the critical need for the development of novel diagnostic and therapeutic strategies that are tailored specifically to address the unique challenges of TNBC.

Advancements in the fields of metabolomics and transcriptomics herald new vistas for elucidating the intricate molecular perturbations characteristic of oncogenesis, with the potential to facilitate the identification of novel biomarkers and therapeutic avenues. Metabolomics, in particular, has emerged as the preeminent technology for the advancement of early diagnosis and the refinement of precision medicine. This approach enables the comprehensive quantification and characterization of low-molecular-weight molecules within biological systems, thereby illuminating potential diagnostic biomarkers and mirroring the underlying biochemical activities and states of cells and tissues [4]. Through the analysis of metabolite profiles from serum, tissue, and cell samples, researchers have identified metabolic disturbances in TNBC patients, including alterations in the glycerophospholipid metabolism pathway, fatty acid metabolism, the tricarboxylic acid (TCA) cycle, and glutathathione biosynthesis pathway [5–8]. However, the results across different biological specimens show significant disparities, highlighting challenges in the credibility and reproducibility of diagnostic biomarkers. This is mainly because the identification of disrupted metabolic pathways in TNBC largely relies on changes in metabolite levels, with only a few biomarkers being validated through other omics approaches. Systems biology focuses on the biological significance of metabolites, advocating for the integration of metabolomics with other omics technologies to elucidate the complex networks of molecular pathways involved in tumorigenesis [9]. Transcriptomics, which interprets the functional components of the genome, contributes valuable insights into the unique biological responses to diseases. The fusion of metabolomics and transcriptomics data has propelled cancer research forward, leveraging advancements in systems biology and bioinformatics [10–12]. Yet, the application of this integrated approach remains underutilized in TNBC research, indicating a significant area for further exploration.

Consequently, the elucidation of the specific aberrant metabolic pathways contributing to the pathogenesis of TNBC necessitates the implementation of a meticulously designed research methodology, underpinned by an integrated analytical framework. The objective of the present investigation is to harness the capabilities of integrated omics technologies to discern differentially expressed metabolites and genes, thereby shedding light on the metabolic pathways that diverge in TNBC from those in HC. By undertaking exhaustive analyses through both metabolomics and transcriptomics, this study endeavors to enhance our comprehension of the metabolic deviations and gene expression alterations characteristic of TNBC. This endeavor aims to lay the groundwork for the identification of novel biomarkers and to foster a deeper understanding of the underlying pathophysiological mechanisms of TNBC.

Materials and methods

Chemical and materials

Methanol and acetonitrile of high performance liquid chromatography (HPLC) grade were procured from Fisher Scientific (Loughborough, UK). Similarly, formic acid, also of HPLC grade, was acquired from TCI (Shanghai, China). The procurement of ammonium acetate, adhering to HPLC grade standards, was facilitated through Sigma-Aldrich (Shanghai, China). The 2-chloro-L-phenylalanine was obtained from Aladdin (Shanghai, China). Furthermore, distilled water was filtered through the Milli-Q system (Millipore, Bedford, USA).

Study design and sample collection

This investigation was conducted at the Second Affiliated Hospital of Fujian Medical University from 2021 to 2022, with ethical approval obtained from the hospital's Ethics Committee under reference number 2021[168]. Prior to the collection of blood specimens, informed consent was duly obtained in written form from all serum donors recruited for participation in the study. TNBC patients ($n=18$) and healthy control (HC) subjects ($n=21$) were initially recruited as a discovery set. The diagnostic criteria for TNBC followed clinical and pathological standards, defined by the absence of estrogen receptor, progesterone receptor, and HER2 expression. Patients had not undergone any therapeutic interventions such as neoadjuvant chemotherapy or radiotherapy. The control subjects were enrolled from the hospital's Physical Examination Center and consisted of healthy, age-matched volunteers with no prior history of breast disease, whose health status was rigorously verified through comprehensive physical exams. Given that the metabolic environment varies along with the formation and progression

of breast cancer, all serum donors were female and free from other diseases such as hypertension, kidney disease, and diabetes. A validation set, consisting of TNBC patients ($n=7$) and HC subjects ($n=5$), was randomly selected and tested using our approach, with inclusion criteria identical to the discovery set.

Blood specimens were procured from fasting participants, and subsequently deposited into tubes specifically engineered for serum segregation. Following a centrifugation process at 3000 rpm for a duration of 5 min at a temperature of 4℃, the serum was successfully isolated. Then, the serum samples were expeditiously transferred to a refrigeration unit maintained at −80 °C, thereby preserving them for future metabolomics analyses.

LC-MS based metabolome profiling

After thawing on ice, 100 μL of the serum was mixed with 400 μL of methanol then vortex-mixed for 1 min. The mixture is then centrifuged at 12,000 rpm for 10 min at 4 ℃ to precipitate proteins. After the supernatant was evaporated to dryness using a centrifugal vacuum evaporator, 150 μL of an 80:20 methanol-water solution (v/v) containing 4 ppm of 2-chloro-l-phenylalanine as an internal standard was added to reconstitute the dried residue. The solution was then filtered through a 0.22 μm membrane, and the resulting filtrate was transferred to an autosampler vial for LC-MS analysis.

In a parallel experimental setup, pooled quality control (QC) samples were prepared by mixing equal volumes of all serum supernatants. These QC samples played a pivotal role in assessing the stability and consistency of the overall experimental outcomes. The pooled QC sample was initially injected five times at the beginning of the analytical batch to equilibrate the column. Furthermore, it was injected once after every six serum sample injections throughout the entire analytical workflow to ensure accuracy.

Chromatographic separations were performed on a Vanquish ultra-high performance liquid chromatography (UHPLC) System (Thermo Fisher Scientific, USA), employing an ACQUITY UPLC® HSS T3 column (150×2.1 mm, 1.8 μm, Waters, Milford, MA, USA) for the analysis. The metabolomic analyses were performed in both electrospray ionization positive (ESI+) and negative (ESI−) ion modes. For ESI+, the mobile phases were composed of A2 (0.1% formic acid in water) and B2 (0.1% formic acid in acetonitrile), with the elution gradient meticulously structured as follows: from 0 to 1 min, the composition was maintained at 2% B2; from 1 to 9 min, it was gradually increased from 2 to 50% B2; from 9 to 12 min, it was further increased from 50 to 98% B2; from 12 to 13.5 min, it was held constant at 98% B2; from 13.5 to 14 min, it was rapidly decreased from 98 to 2% B2; and finally, from 14 to 20 min, it was

maintained at 2% B2. In the ESI- mode, the mobile phases comprised A3 (ammonium formate at 5 mM) and B3 (acetonitrile), with the elution conditions set as follows: from 0 to 1 min, the composition was at 2% B3; from 1 to 9 min, it was increased from 2 to 50% B3; from 9 to 12 min, it was raised from 50 to 98% B3; from 12 to 13.5 min, it remained at 98% B3; from 13.5 to 14 min, it was decreased from 98 to 2% B3; and from 14 to 17 min, it was kept at 2% B3. The column oven temperature was uniformly maintained at 40 °C, with a flow rate of 0.25 mL/min and an injection volume of 2 μL. Throughout the duration of the experiment, all pre-treated serum samples were preserved at 4 °C.

Metabolite detection was facilitated through a Q Exactive HF-X mass spectrometer (Thermo Fisher Scientific, USA), which was equipped with an ESI ion source and operated in both MS1 and MS/MS (Full MS-ddMS2 mode, data-dependent MS/MS) acquisition modes. The operational parameters were meticulously defined, with sheath gas pressure set at 30 arb, auxiliary gas flow at 10 arb, spray voltages calibrated at 3.50 kV for ESI(+) and −2.50 kV for ESI(−), capillary temperature at 325℃, MS1 scan range from m/z 81 to 1000, MS1 resolving power at 60,000 FWHM, eight data-dependent scans per cycle, MS/MS resolving power at 15,000 FWHM, normalized collision energy at 30%, and dynamic exclusion time set to automatic.

Metabolomics data analysis

The transformation of raw data into mzXML format was accomplished utilizing MSConvert, a component of the ProteoWizard software suite (version 3.0.8789) [13]. Then, the feature detection, retention time correction, and alignment of the data were executed through the application of XCMS. Subsequently, advanced multivariate statistical analyses, namely principal component analysis (PCA) and orthogonal partial least squares-discriminant analysis (OPLS-DA) were conducted using Simca-P14.1 software. These analyses served to delineate distinct groups and pinpoint biomarkers indicative of TNBC. To ascertain the robustness of the model, a permutation test encompassing 100 random permutations was employed, evaluating the OPLS-DA model based on its R^2 (explained variance) and Q^2 (predictive ability) parameters. The identification of discriminating metabolites was facilitated by the OPLS-DA model through the implementation of the variable importance on projection (VIP) strategy, whereby only metabolites exhibiting a VIP value over 1 were deemed to possess statistical significance in the classification of TNBC. Following this, a nonparametric univariate statistical analysis was conducted, employing the Mann-Whitney U test ($p<0.05$) in conjunction with fold change (FC) values ≤0.67 or ≥1.5 to discern differential metabolites (DMs).

The evaluation of the DMs' predictive capacity was undertaken through receiver operating characteristic (ROC) curve analysis, which leveraged the area under the ROC curve (AUC) as an indicator of the overall test efficacy. The optimal cut-off values of the DMs based on the ROC curve were determined by the Youden index, calculated as sensitivity+specificity −1 [4]. The DeLong test was applied to compare AUCs. All the analyses were performed using SPSS software (version 26).

The initial identification of DMs was predicated on the verification of accurate molecular weight (<30 ppm). After that, an analysis was conducted using accurate mass numbers and high-resolution target MS/MS spectra, along with the fragmentation laws for various metabolites. The exploration for potential structures of DMs was conducted through database searches (including METLIN, HMDB, and MassBank) and literature reviews, thereby accruing information on candidate metabolites.

Furthermore, Metabolite Set Enrichment Analysis (MSEA) was performed via MetaboAnalyst 6.0 (https://metascape.org/gp/index.html), aimed at elucidating metabolic pathways distinctly altered in TNBC patients in comparison to HC subjects.

Transcriptomics analysis

In the investigation of TNBC, three pertinent datasets from the Gene Expression Omnibus (GEO) database were meticulously selected for analysis: GSE65194, encompassing 55 TNBC tissue samples alongside 11 samples of healthy breast tissue derived from mammoplasty procedures; GSE45827, comprising 11 TNBC and 5 healthy breast tissue samples; and GSE36295, containing 41 TNBC tissues as well as 11 samples of normal tissue. The identification of differentially expressed genes (DEGs) contrasting the TNBC group with the group of normal breast tissues was executed utilizing the GEO2R analytical tool, adhering to stringent cutoff criteria of an absolute log2 FC greater than 2 and an adjusted *p*-value less than 0.05. This initial analysis facilitated the generation of volcano plots and Venn diagrams, accessible via (http://www.bioinformatics.com.cn/), to discern DEGs consistently observed across the trio of datasets.

After identifying the shared DEGs, gene ontology (GO) enrichment analysis and Kyoto Encyclopedia of Genes and Genomes (KEGG) pathway enrichment analysis were conducted using the Database for Annotation, Visualization, and Integrated Discovery (DAVID, version 12.0). The GO enrichment analysis was categorized into three aspects: biological process (BP), cellular component (CC), and molecular function (MF). BP represents a sequence of coordinated molecular functions that achieve a specific biological goal, CC refers to the cellular locations where gene products are active, and MF describes the biochemical activities of gene products at the molecular level.

After identifying shared DEGs, gene ontology (GO) enrichment analysis and Kyoto Encyclopedia of Genes and Genomes (KEGG) pathway enrichment analysis were conducted using the Database for Annotation, Visualization, and Integrated Discovery (DAVID, version 12.0). The GO enrichment analysis was divided into three categories: biological process (BP), cellular component (CC), and molecular function (MF). BP refers to a series of events or molecular functions coordinated to achieve a biological objective. CC indicates the cellular location where gene products are active, while MF describes the biochemical activities of gene products at the molecular level. This multifaceted approach aimed to elucidate the underlying molecular mechanisms and potential pathophysiological pathways relevant to TNBC, providing valuable insights into the biological characterization of this aggressive breast cancer subtype.

Joint analysis of metabolomics and transcriptomics

An integrative analysis was undertaken to explore the synergistic relationship between DMs and DEGs, as identified through comprehensive metabolomic and transcriptomic investigations. This analysis was conducted by employing the Joint-Pathway Analysis module available within the MetaboAnalyst 6.0 platform, aimed at constructing a detailed metabolic pathway enrichment diagram. The analysis leveraged the total number of identified metabolites to evaluate the relevance and significance of each pathway, with pathways demonstrating a *p*-value less than 0.05 being deemed significantly enriched. In parallel, the KEGG database served as a pivotal resource for elucidating potential genes implicated within these significantly enriched pathways. The utilization of Cytoscape software version 3.9.1, in conjunction with the Metscape plugin, facilitated the elucidation of the intricate connections between metabolites and genes, thereby enabling the visualization of compound networks.

Validation of the expression of hub DEGs from the online dataset

Gene Expression Profiling Interactive Analysis (GEPIA; http://gepia.cancer-pku.cn/) represents a sophisticated interactive web service dedicated to the analysis of RNA sequencing expression data, incorporating 9,736 tumor and 8,587 normal samples derived from the Cancer Genome Atlas (TCGA) and the Genotype-Tissue Expression (GTEx) projects [14]. Concurrently, UALCAN (http://ualcan.path.uab.edu) emerges as an extensive, intuitive web portal tailored for the analysis of cancer OMICS data. This portal not only facilitates gene expression analysis predicated on clinical data from TCGA but

also extends its functionality to include protein expression analysis leveraging data from the Clinical Proteomic Tumor Analysis Consortium (CPTAC) Confirmatory/ Discovery dataset [14, 15]. Furthermore, the Human Protein Atlas (HPA) database (https://www.proteinatlas.org) provides an invaluable open-access repository of immunohistochemical images, documenting a broad spectrum of immune response observations across both neoplastic and normal tissues [16]. Employing the comprehensive datasets available within these repositories, a detailed comparative analysis of the mRNA and protein expressions of key hub genes in breast cancer versus normal breast tissue was conducted, with immunohistochemistry serving as the foundational analytical technique.

Cell culture

The human breast cancer cell line MDA-MB-231 and the non-tumorigenic breast epithelial cell line MCF-10 A were obtained from the American Type Culture Collection (ATCC). MDA-MB-231 cells were cultured in low-glucose Dulbecco's Modified Eagle's Medium (DMEM) supplemented with 10% fetal bovine serum (FBS). MCF-10 A cells were cultured in DMEM/F12 medium supplemented with 5% horse serum, 20 ng/mL epidermal growth factor (EGF), 10 μg/mL insulin, and 0.5 μg/mL hydrocortisone. All cells were maintained in a humidified incubator with 5% CO_2 at 37 ℃.

Western blot analysis

Cells were harvested and subsequently lysed in RIPA buffer containing protease inhibitors (Roche Ltd, Basel, Switzerland). Protein concentrations were quantified using the Micro BCA protein assay kit (Pierce Biotechnology). Protein samples were separated by 10% SDS-PAGE and transferred to Amersham Protran nitrocellulose membranes (GE Healthcare Life Sciences, Fairfield, USA). The membranes were incubated overnight at 4℃ with specific primary antibodies diluted in blocking solution. The antibodies used included anti-MAOA (1:600, Proteintech, 10539-1-AP), anti-ADH1B (1:2200, Proteintech, 66939-1-Ig), anti-ADH1C (1:400, Proteintech, 18897-1-AP), anti-AOC3 (1:2400, Proteintech, 66834-1-Ig), anti-PCK1 (1:650, Proteintech, 16754-1-AP), and anti-GAPDH (1:5000, Immunoway, YM3029). Immunoreactive bands were visualized and quantified using the Odyssey® CLx Infrared Imaging System (LI-COR Biosciences).

Kaplan-Meier plotter database analysis

The Kaplan-Meier plotter database (www.kmplot.com) was deployed to elucidate the association between mRNA levels of each pivotal DEG and the prognostic outcomes of patients afflicted with TNBC. To this end, patient samples were stratified into two distinct groups predicated upon the median expression level of each gene, delineating cohorts with high versus low expression, thereby facilitating a rigorous evaluation of the prognostic relevance attributed to each gene. Notably, the platform autonomously computes the hazard ratios (HR) accompanied by 95% confidence intervals (CI) and Log rank P values, thereby streamlining the analytical process.

Results

General characteristics of study participants

In the current investigation, the cohort comprised exclusively female subjects, with an established homogeneity in age demographics across all study groups. To minimize the potential confounding impact of variables such as age, homogeneity within each group was rigorously evaluated utilizing the Kruskal-Wallis test. The participant pool included a total of 51 individuals: the discovery set consisted of 18 patients diagnosed with TNBC (age 47 [range 27–59] years) and 21 HC (age, 46 [range 33–66] years), whereas the validation set encompassed 7 TNBC patients (age 51 [range 36–58] years) and 5 HC (age, 50 [range 39–63] years). Analysis revealed no significant disparities in baseline characteristics among the groups, thereby reinforcing the internal validity of the study findings.

The metabolomics analysis for TNBC and HC serum samples

Reliability of the analytical method

In this study, multivariate statistical analyses were initially utilized to construct metabolic profiles for the entirety of the samples under study. The reliability of this analytical method was rigorously evaluated through the systematic repetition of analyses on QC samples across all sample runs. Subsequently, the PCA score plots for the samples within the discovery dataset were examined. Notably, all QC samples (Fig. 1, yellow) exhibited a pronounced clustering in both ESI+and ESI- modes. This observation unequivocally confirms the analytical system's stability and reproducibility.

Differential metabolite screening

As shown in Fig. 1, the PCA score plots exhibited well-distinguishable patterns between TNBC and HC samples, implying some remarkable differences existed in the serum endogenous metabolites between the two different groups. Building on this initial finding, OPLS-DA was applied to further pinpoint these metabolic discrepancies. The results (Fig. 2A, B) demonstrated clear division between the two groups, with impressive R^2Y and Q^2 values of 0.984 and 0.878 in ESI+mode, and 0.995 and 0.834 in ESI- mode, respectively. Subsequently, the results from 100 permutation tests revealed that the permuted R^2 and Q^2 values on the left side were consistently lower than the
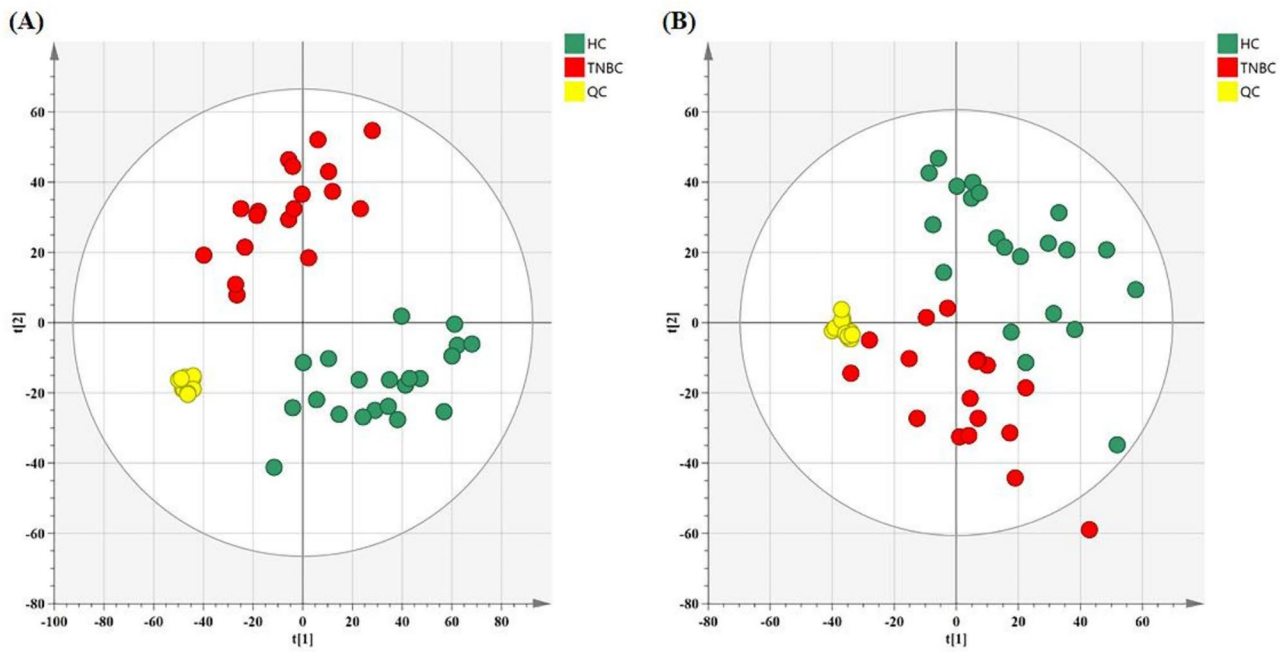
Fig. 1 PCA score plots of samples in the discovery set and QCs (HC: green; TNBC patients: red; QC: yellow) in (**A**) positive and (**B**) negative electrospray ionization mode
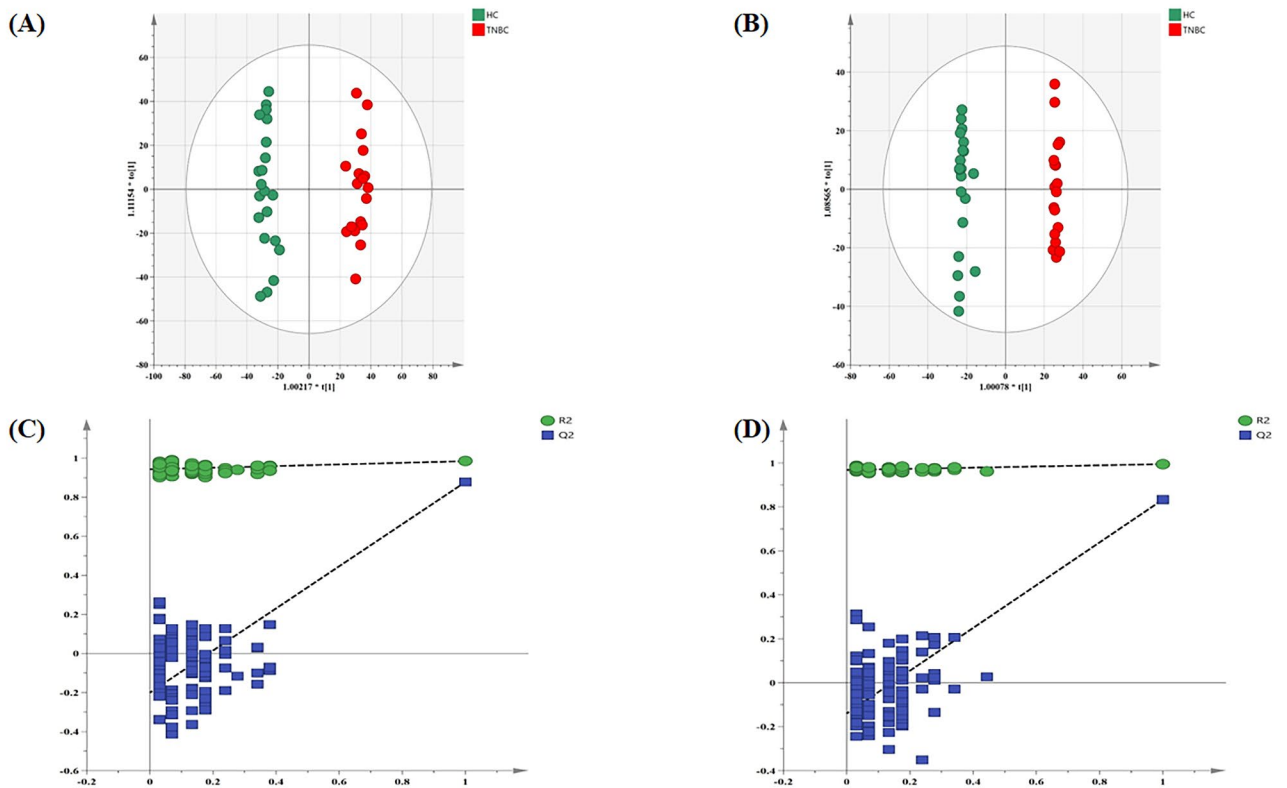
Fig. 2 The OPLS-DA score plots of the two groups revealed the clustering of samples in the discover set and their corresponding permutation tests. OPLS-DA score plots for HC (green, *n* = 21) and TNBC (red, *n* = 18) in (**A**) ESI+ mode and (**B**) ESI- mode. The corresponding validation plots for putative features with 100 permutation tests in (**C**) ESI+ mode and (**D**) ESI- mode

original values on the right side, indicating no overfitting of the model (Fig. 2C, D). Furthermore, the intercept of Q^2 being below zero further supports the model's reliability and validity [17].

In this work, after the application of predefined criteria, a total of 22 DMs were identified as potential biomarkers for differentiating between TNBC and HC specimens. The comparative analysis elucidated that within the TNBC cohort, there were 13 metabolites exhibiting upregulation and 9 demonstrating downregulation in contrast to the HC group. The concentration profiles of these 22 DMs were systematically represented in a heat map (Supplementary Fig. 1), while comprehensive details encompassing retention time (RT), mass-to-charge ratio (m/z), adduct ion, FC, *p*-value, VIP, and mean decrease accuracy were listed in Table 1.

Evaluating and validating the diagnostic ability of metabolites

To ascertain the diagnostic potential of specific metabolites, ROC analysis was employed to assess the diagnostic accuracy of individual metabolites. The range of AUC was between 0.5 and 1, with values closer to 1 indicating higher accuracy of the detection method, while values closer to 0.5 indicating lower accuracy and lower application value [18]. This analysis yielded that 7 DMs manifested statistically significant diagnostic capabilities ($p < 0.001$), namely 7-methylguanine, pipecolic acid, L-methionine, oxoglutaric acid, bilirubin, thymidine, and

4-hydroxyphenylacetaldehyde (Supplementary Fig. 2). Using DeLong's test, we found that 7-methylguanine demonstrated significantly better diagnostic power than oxoglutaric acid, bilirubin, thymidine, and 4-hydroxyphenylacetaldehyde ($p < 0.05$). However, there was no significant difference in the AUC between the other biomarkers ($p > 0.05$). The precise *p*-values from DeLong's test comparing the AUCs of these biomarkers are provided in Supplementary Table S1. These results revealed that 7-methylguanine in serum samples exhibited the highest efficacy in distinguishing TNBC patients from HC subjects, with an AUC of 0.992, sensitivity of 100%, specificity of 95.2%, and a Youden index of 0.952.

To corroborate the results obtained from the initial discovery set, serum samples were procured from 7 individuals diagnosed with TNBC and 5 HC. These samples underwent analysis employing identical UHPLC–MS procedures as those utilized for the discovery set. The relative intensity of 7-methylguanine between TNBC patients and healthy individuals was compared in the discovery set and replication set, respectively. Findings demonstrated a significant elevation of 7-methylguanine levels in the serum samples of TNBC patients in both discovery and validation sets ($p < 0.01$; Fig. 3A), indicating a consistent elevation of this metabolite in the context of TNBC.

Subsequently, to ascertain the diagnostic utility of 7-methylguanine within a clinical setting, ROC curves were generated based on the relative intensity of

Table 1 Serum differential metabolites detected by UHPLC-MS between TNBC and HC subjects

No.	Metabolites	Rt(s)	mz	formula	KEGG	Adduct ion	FC	P	VIP
1	Isonicotinic acid	600.2	122.0217	C6H5NO2	C07446	[M-H]-	0.54	0.036	1.464
2	Ergothioneine	102.7	230.096	C9H16N3O2S	C05570	[M+H]+	0.54	0.006	1.546
3	Glutaric acid	86.1	131.0329	C5H8O4	C00489	[M-H]-	0.55	0.005	1.555
4	Urocanic acid	139.1	137.0345	C6H6N2O2	C00785	[M-H]-	0.58	0.003	1.730
5	Acetylcholine chloride	33	180.9729	C7H16NO2. Cl	C08201	[M-H]-	0.58	0.005	1.767
6	2,3-Butanediol	152.6	154.9901	C4H10O2S2	C00265	[M+H]+	0.59	0.011	1.036
7	5'-Methylthioadenosine	897.2	297.2429	C11H15N5O3S	C00170	[M-H]-	0.6	0.024	1.705
8	N-Acetyl-D-tryptophan	397.1	246.1238	C13H14N2O3	C03137	[M+H]+	0.61	0.001	1.715
9	9(S)-HPOT	855.1	293.2108	C18H30O4	C16321	[M+H]+	0.65	0.006	1.429
10	4-Hydroxyphenylacetaldehyde	95.1	136.048	C8H8O2	C03765	[M+H]+	1.5	0.000	1.851
11	7-Methylguanine	139.6	166.0724	C6H7N5O	C02242	[M+H]+	1.53	0.000	2.406
12	Thymidine	539.7	242.1759	C10H14N2O5	C00214	[M-H]-	1.58	0.000	1.987
13	Oxalacetic acid	83.1	130.9993	C4H4O5	C00036	[M-H]-	1.59	0.029	1.572
14	CMP-3-deoxy-D-manno-octulosonate	773	542.1068	C17H26N3O15P	C04121	[M-H]-	1.62	0.006	1.421
15	Oxoglutaric acid	75.8	145.0137	C5H6O5	C00026	[M-H]-	1.66	0.000	2.237
16	Bilirubin	917.5	585.2655	C33H36N4O6	C00486	[M+H]+	1.7	0.000	1.731
17	Thymine	430.5	125.0347	C5H6N2O2	C00178	[M-H]-	1.71	0.047	1.288
18	L-Valine	135.2	118.087	C5H11NO2	C00183	[M+H]+	1.73	0.015	1.018
19	Arachidic acid	917.3	311.2954	C20H40O2	C06425	[M-H]-	1.75	0.003	1.581
20	(S)-4-Hydroxymandelate	245.5	151.0336	C8H8O4	C03198	[M+H]+	1.85	0.007	1.121
21	Pipecolic acid	96.9	129.0654	C6H11NO2	C00408	[M+H]+	2.14	0.000	1.646
22	L-Methionine	137.4	148.0426	C5H11NO2S	C00073	[M-H]-	2.49	0.000	2.285
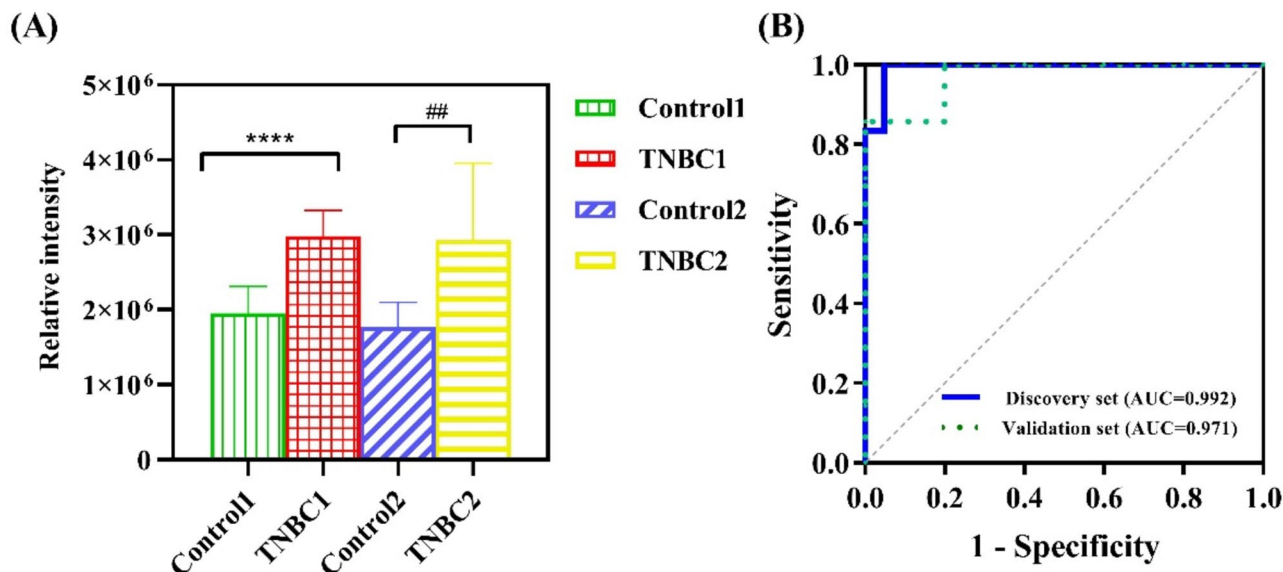
Fig. 3 Validation of the diagnostic efficacy of 7-Methylguanine for discriminating between TNBC and HC groups across discovery set and validation sets. (**A**)> Comparative analysis of 7-methylguanine levels (****$p < 0.0001$ in the discovery set; ## $p < 0.01$ in the validation set). Control1 and TNBC1 represent HC subjects ($n = 21$) and TNBC patients ($n = 18$) of the discovery set, respectively. Control2 and TNBC2 represent HC subjects ($n = 5$) and TNBC patients ($n = 7$) of the validation set, respectively. (**B**) ROC curve analysis for diagnostic accuracy

metabolites derived from the validation sample cohort. Within this validation set, 7-methylguanine exhibited an AUC of 0.971, with a sensitivity of 85.7% and specificity of 100%, corresponding to a Youden index of 0.857. These metrics closely paralleled those observed within the discovery set (Fig. 3B), reinforcing the potential of 7-methylguanine as a robust biomarker for TNBC.

Metabolite set enrichment analysis (MSEA)
The findings indicate that TNBC is characterized by distinct metabolite profiles, implying alterations in metabolic biological networks. To delineate the disrupted metabolic pathways, informed by the altered set of DMs, comprehensive enrichment and pathway analyses were undertaken. The analyses revealed that the most significantly enriched pathways in TNBC patients include the malate-aspartate shuttle, alanine metabolism, spermidine and spermine biosynthesis, urea cycle, ammonia recycling, TCA cycle, gluconeogenesis, and aspartate metabolism, all of which demonstrated statistical significance (p-values < 0.05) as depicted in the bar chart in Supplementary Fig. 3.

The transcriptomics analysis for TNBC and HC tissue samples
#### *Identification of differentially expressed genes in TNBC*
In this study, three GEO datasets were scrutinized: GSE65194, GSE45827, and GSE36295. To ensure the dataset's quality is reliable, a rigorous analytical approach was employed using the GEO2R tool, with selection criteria set at an absolute log fold change (|logFC|)

exceeding 2 and an adjusted *p*-value below 0.05. This analysis yielded that, compared to normal breast tissue, TNBC tissue had 1,561 up-regulated and 1,035 down-regulated DEGs in the GSE65194 dataset (Fig. 4A), 1,533 up-regulated and 1,047 down-regulated DEGs in GSE45827 (Fig. 4B), and 77 up-regulated along with 137 down-regulated DEGs in GSE36295 (Fig. 4C). After the identification of DEGs within each dataset, an online Venn diagram tool was employed to intersect and visualize the DEGs across the three datasets, facilitating the identification of common DEGs. This analysis revealed a total of 160 DEGs demonstrating uniform expression trends across the datasets, encompassing 57 genes that were up-regulated and 103 that were down-regulated, as depicted in Fig. 4D.

Gene ontology and KEGG enrichment functional analysis of overlapping DEGs
To examine the biological categorization of the 160 common DEGs, functional and pathway enrichment analyses were executed utilizing the DAVID database. These investigations comprised GO enrichment analysis and KEGG pathways, which disclosed associations of the DEGs with 39 GO terms including BP, CC, and MF, in addition to 2 significant pathways, as listed in Supplementary Table S2. The threshold for deeming results statistically significant was established at a False Discovery Rate (FDR) below 0.05. As depicted in Fig. 5A, the GO analysis explicitly highlighted that DEGs about BP were notably concentrated in areas such as cell division, mitotic spindle organization, bacterial response,
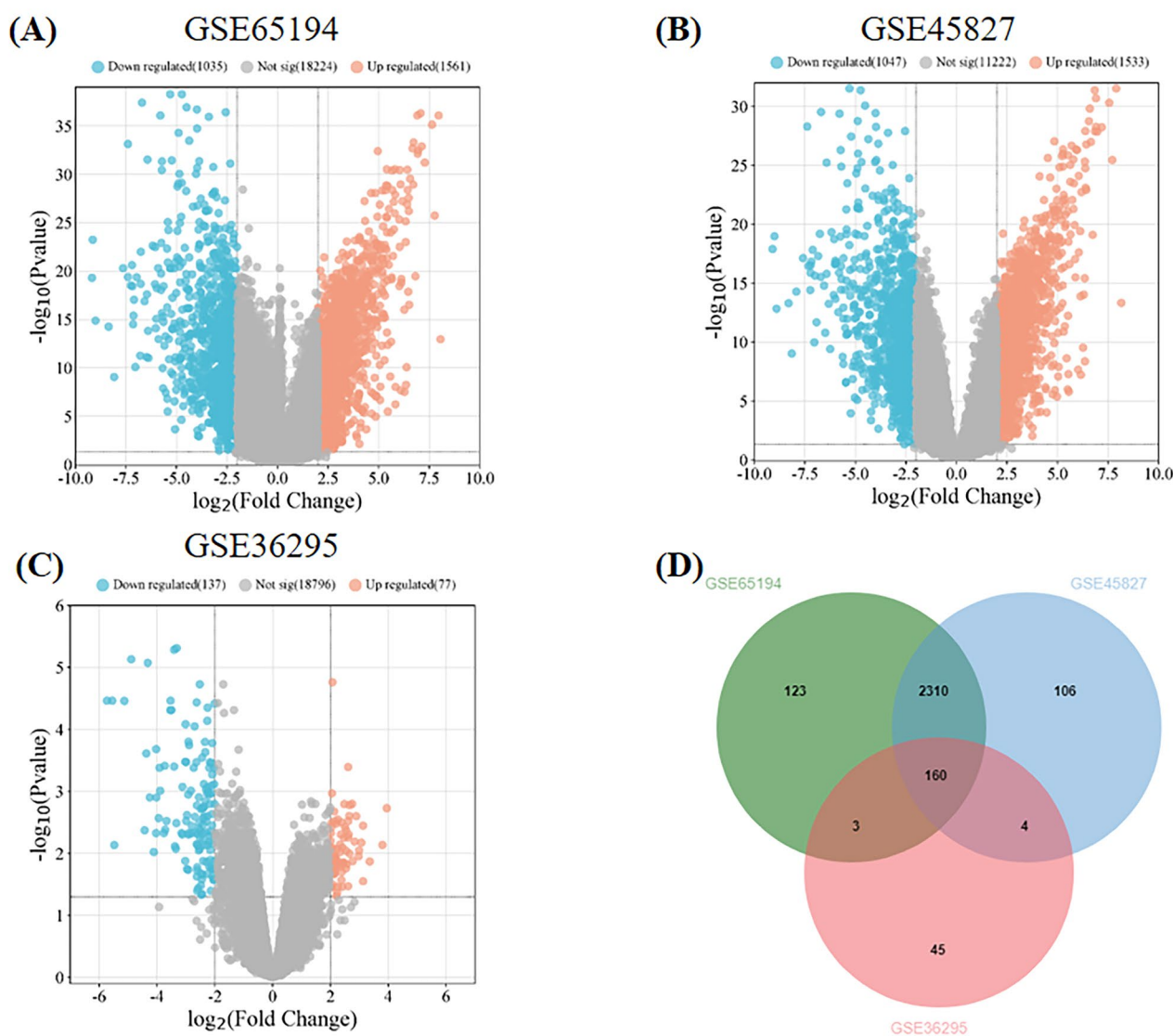
Fig. 4 Identification of overlapping DEGs. Volcano plots for DEGs in TNBC and normal tissues based on data from GEO datasets (**A**) GSE65194, (**B**) GSE45827, and (**C**) GSE36295. (**D**) Venn diagrams of the DEGs from the three data sets. Different colors in the figure mean different data sets

and so on. For CC, significant enrichment was observed in structures including the midbody, spindle, and condensed chromosome outer kinetochore. Furthermore, changes in MF were mainly enriched in microtubule binding. Regarding the KEGG pathway analysis, the DEGs were predominantly enriched in the PPAR signaling pathway and tyrosine metabolism (Fig. 5B).

Integrative analysis of metabolomics and transcriptomics data

To advance the systematic exploration of TNBC, a comprehensive biological pathway analysis was performed by linking important 22 DMs and the 160 DEGs through shared metabolic pathways with the Joint Pathway Analysis module on MetaboAnalyst 6.0. Our analysis unveiled

three pathways of notable perturbation: tyrosine metabolism, phenylalanine metabolism, and glycolysis or gluconeogenesis, each characterized by p-values < 0.05 and impact ≥ 0.5 (Fig. 6A; Table 2). To better understand the metabolite mechanism and gene dysregulation, 22 DMs and 160 DEGs were introduced into the Metscape plugin of the Cytoscape 3.7.1 database to collect the compound–reaction–enzyme–gene network in combination with the top three enriched pathways (Fig. 6B). The results showed that six key genes linked to these pathways, with detailed information listed in Table 3.

Verifications of six hub genes expression

Upon integrating the outcomes derived from metabolomics and transcriptomics datasets, this study identified
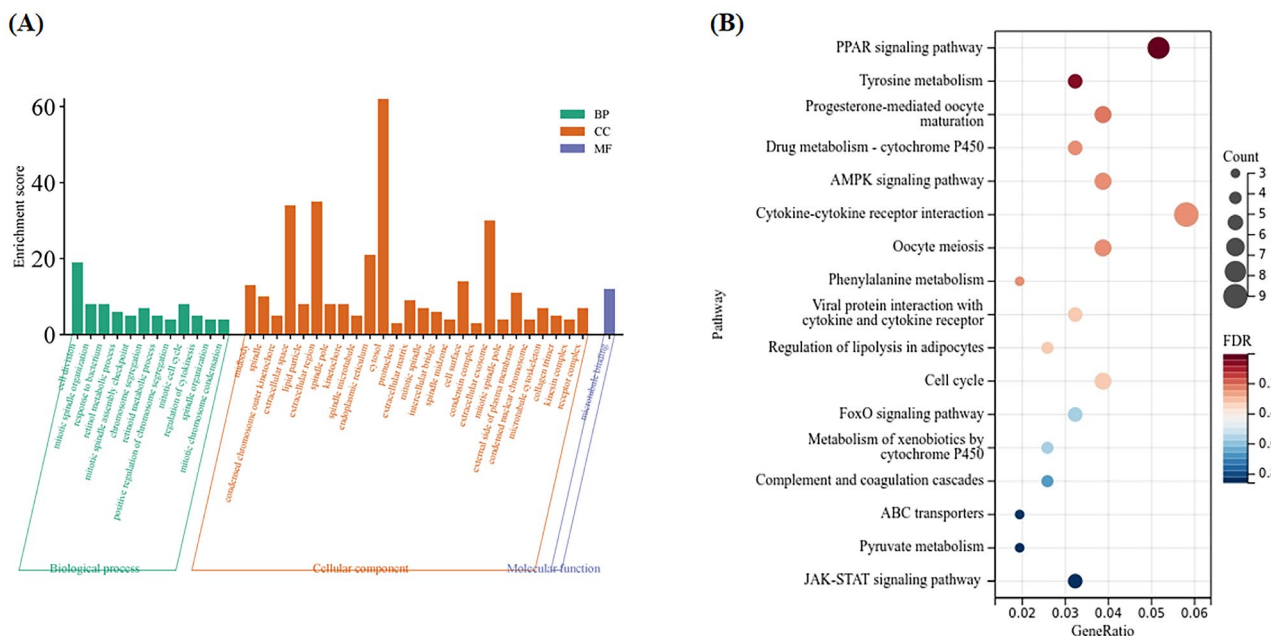
Fig. 5 DAVID analysis of the overlapping DEGs. **(A)** GO and **(B)** KEGG enrichment analyses of the common DEGs. The size of the node reflects the count of genes enriched in terms, and the color shows the P value, the redder the color, the more significant it is. DAVID, Database for Annotation, Visualization, and Integrated Discovery; DEGs, differentially expressed genes; GO, gene ontology; KEGG, Kyoto Encyclopedia of Genes and Genomes
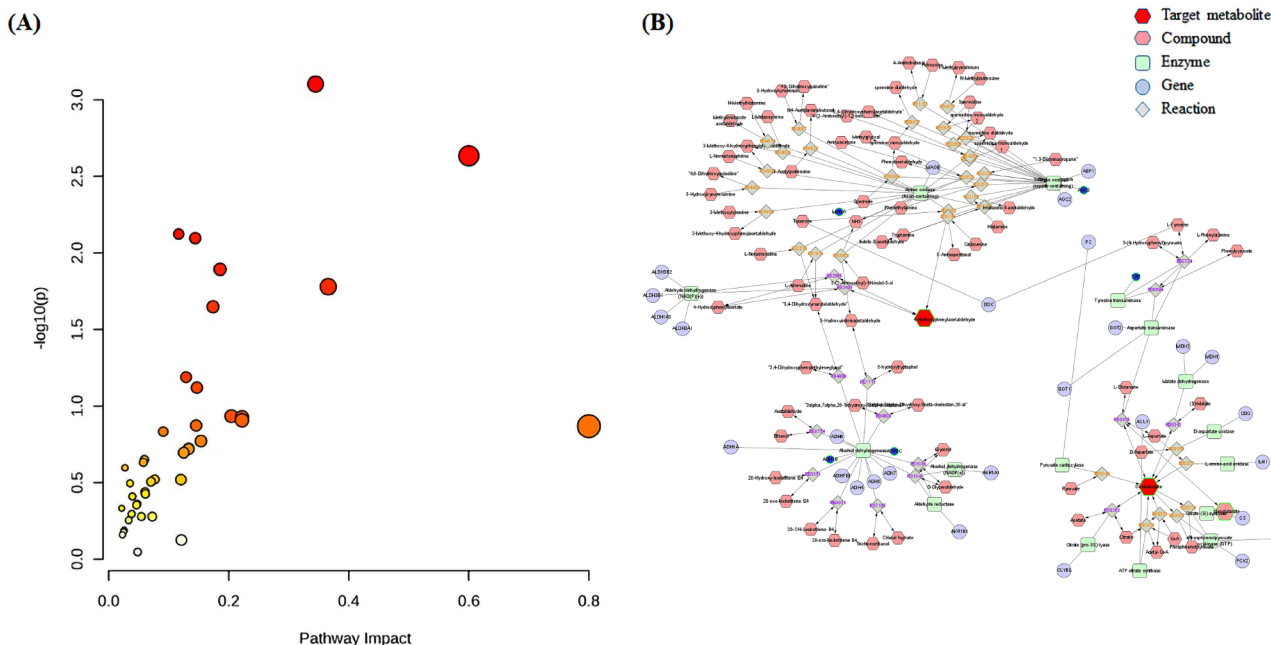
Fig. 6 Integrated transcriptomics and metabolomics analyses of TNBC metabolic pathways. **(A)** Metabolic pathway enrichment plot. **(B)** The compound–reaction–enzyme–gene network of the key metabolites and genes. Significant overexpression in red, significant downexpression in blue

Table 2 Joint analysis pathways of differential metabolites and genes

No	Pathway name	Match status	*P* value	Impact
1	Tyrosine metabolism	6/88	0.001	0.345
2	Phenylalanine metabolism	3/21	0.002	0.600
3	Glycolysis or Gluconeogenesis	4/61	0.008	0.117

MAOA, ADH1B, ADH1C, AOC3, TAT, and PCK1 as potential key players in the pathogenesis of TNBC.

Utilizing the GEPIA platform, we assessed the mRNA expression levels of six pivotal genes in a dataset comprising 135 TNBC specimens and 291 normal breast tissue specimens. This dataset was collated from the

Table 3 Related differentially expressed genes by joint-pathway analysis

Gene	FC	FDR	log2 FC	Gene description	Enriched pathway
MAOA	0.086	4.87E-05	-3.54	monoamine oxidase A	Tyrosine metabolism, Phenylalanine metabolism, Drug metabolism - cytochrome P450
ADH1B	0.0188	3.44E-05	-5.73	"alcohol dehydrogenase 1B (class I), beta polypeptide"	Tyrosine metabolism, Glycolysis or Gluconeogenesis, Drug metabolism - cytochrome P450
ADH1C	0.0501	8.43E-06	-4.32	"alcohol dehydrogenase 1 C (class I), gamma polypeptide"	Tyrosine metabolism, Glycolysis or Gluconeogenesis, Drug metabolism - cytochrome P450
AOC3	0.187	0.00471	-2.42	"amine oxidase, copper containing 3 (vascular adhesion protein 1)"	Tyrosine metabolism, Phenylalanine metabolism
TAT	0.123	0.0132	-3.02	tyrosine aminotransferase	Tyrosine metabolism, Phenylalanine metabolism
PCK1	0.155	0.00257	-2.69	phosphoenolpyruvate carboxykinase 1 (soluble)	Glycolysis or Gluconeogenesis

comprehensive resources of the TCGA and GTEx databases. This examination revealed a statistically significant reduction in the expression of these genes in TNBC in comparison to normal samples ($p < 0.05$, Fig. 7). At the protein level, the UALCAN cancer database showed that their expression in TNBC tissue was significantly reduced relative to normal tissue ($p < 0.05$, Fig. 8A). Moreover, the western blot analysis (Fig. 8B) also indicated that MAOA, ADH1B, ADH1C, AOC3, and PCK1 protein levels were decreased in the MDA-MB-231 cell lines compared to those in the MCF-10 A cell lines. Then, these observations were further substantiated by immunohistochemical analyses sourced from the HPA database. The representative immunohistochemistry (IHC) images in Fig. 9 showed that the expression levels of MAOA, ADH1B, ADH1C, AOC3, and PCK1 were downregulated in breast cancer tissues compared to normal tissues.

Specifically, the analysis included 3 normal samples and 11 cancer samples for MAOA and AOC3, 2 normal samples and 11 cancer samples for ADH1B and ADH1C, and 2 normal samples and 12 cancer samples for PCK1.

**The survival analysis of hub genes in TNBC**

The Kaplan-Meier Plotter, an accessible online analytical tool, was utilized to conduct survival analyses predicated on gene expression levels, thereby evaluating the prognostic relevance of key genes. This analysis divided TNBC patient samples into dichotomous groups based on median mRNA expression levels of each gene, delineating cohorts with high versus low expression. Notably, AOC3 and PCK1 were identified as genes significantly associated with poor overall survival (OS). Results showed that overexpression of AOC3 (HR 95%CI=3.56 (1.62–7.8), log-rank P=0.00073) and PCK1 (HR 95%CI=2.86 (1.19–6.85), log-rank P=0.04) were associated with unfavorable OS of TNBC patients (Fig. 10). Consequently, this evidence supports the hypothesis that AOC3 and PCK1 may function as potential biomarkers for prognostication in TNBC patient populations. Based on these results, it is hypothesized that AOC3 and PCK1 may serve as potential biomarkers for predicting the prognosis of TNBC patients.

Discussion

TNBC is recognized as the most lethal subtype of BC characterized by low OS rates and high rates of a high propensity for invasion and metastasis, posing an unmet medical challenge [19]. Clinical tumor markers such as carcinoembryonic antigen (CEA) and cancer antigen 15−3 (CA15-3) are frequently used in BC diagnosis; nevertheless, their specificity and accuracy do not meet clinical standards [20]. Currently, there are no reliable biomarkers specifically for TNBC, highlighting a critical gap in diagnostic tools. Metabolic reprogramming, a hallmark of cancer, offers new prospects for cancer detection, prognosis, and treatment [21, 22]. It has been demonstrated that metabolic dysregulation is linked to therapy response and clinical outcome across various cancer types and may influence the tumorigenesis, progression, and prognosis of BC via pathways related to angiogenesis, anti-apoptosis, mitogenesis, chronic inflammation, increased visceral fat reserves, and other cancer-associated adipokines [23–26]. This study aims to identify more reliable and specific serum markers for diagnosing TNBC using a metabolomic approach. While metabolomics has been applied in numerous studies to discover novel biomarkers for TNBC, relying solely on this method does not fully elucidate the pathophysiology of TNBC. Therefore, this research integrated metabolomics and transcriptomics data to deepen our understanding of
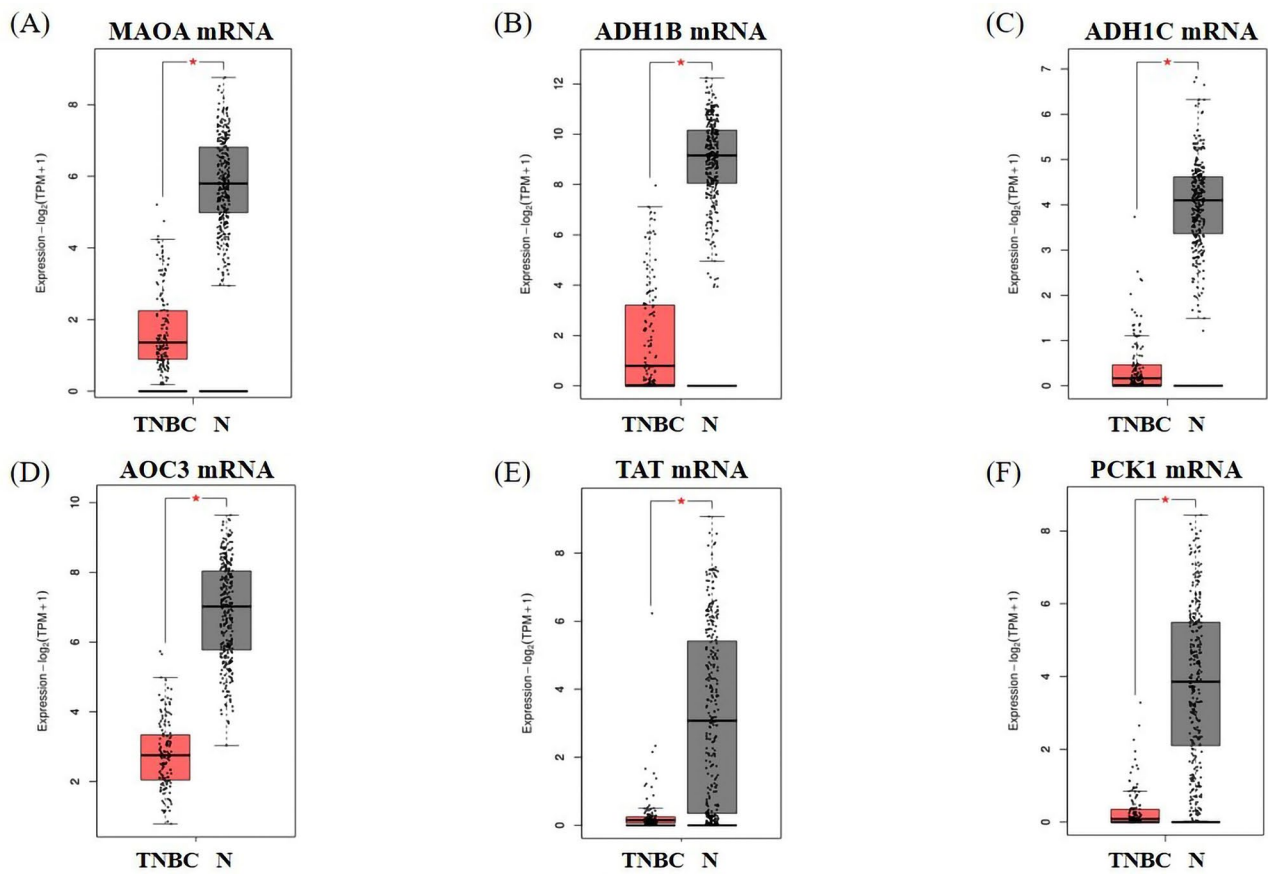
Fig. 7 Significantly expressed six genes in TNBC samples compared to normal samples. (**A**)MAOA, (**B**)ADH1B, (**C**)ADH1C, (**D**)AOC3, (**E**)TAT, and (**F**)PCK1 have notable low mRNA expression in the TNBC specimen compared to the normal specimen (*$p < 0.05$). Red color refers to TNBC tissues and grey color refers to normal samples
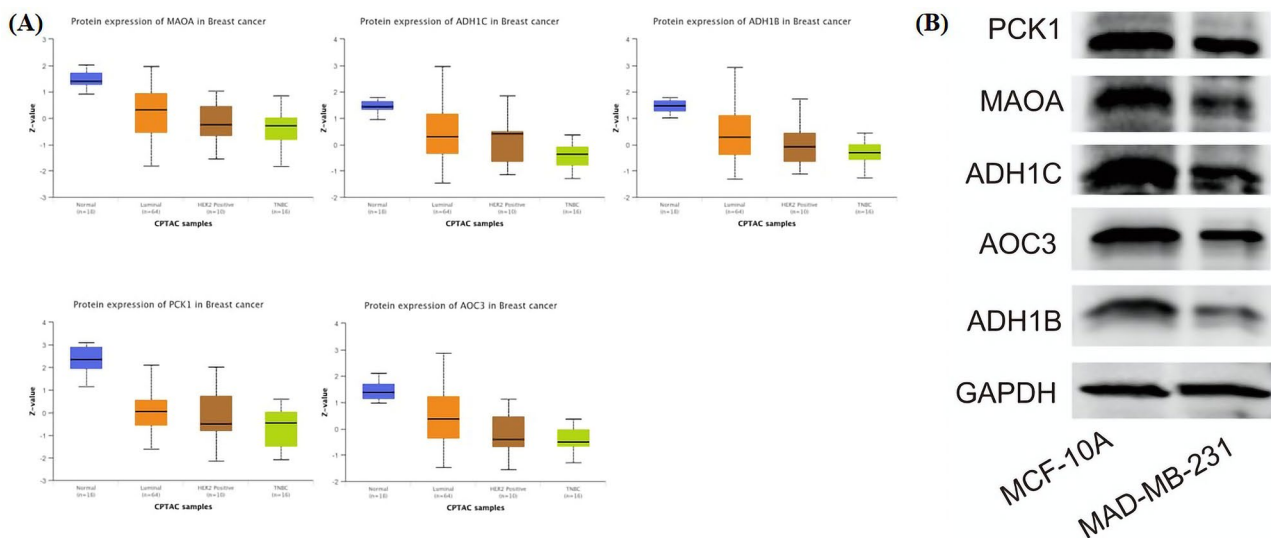

Fig. 8 Protein levels of MAOA, ADH1B, ADH1C, AOC3 and PCK1. (**A**) The protein expression of key genes in normal tissues and breast cancer tissues based on subclasses analyzed by the UALCAN cancer database. Z-values show standard deviations for the specified cancer type from the median across samples. Values for the Log2 Spectral count ratio obtained from CPTAC were first normalized within each sample profile and then across samples. (**B**) The protein expression of key genes in MCF-10 A and MDA-MB-231 cells detected by western blot
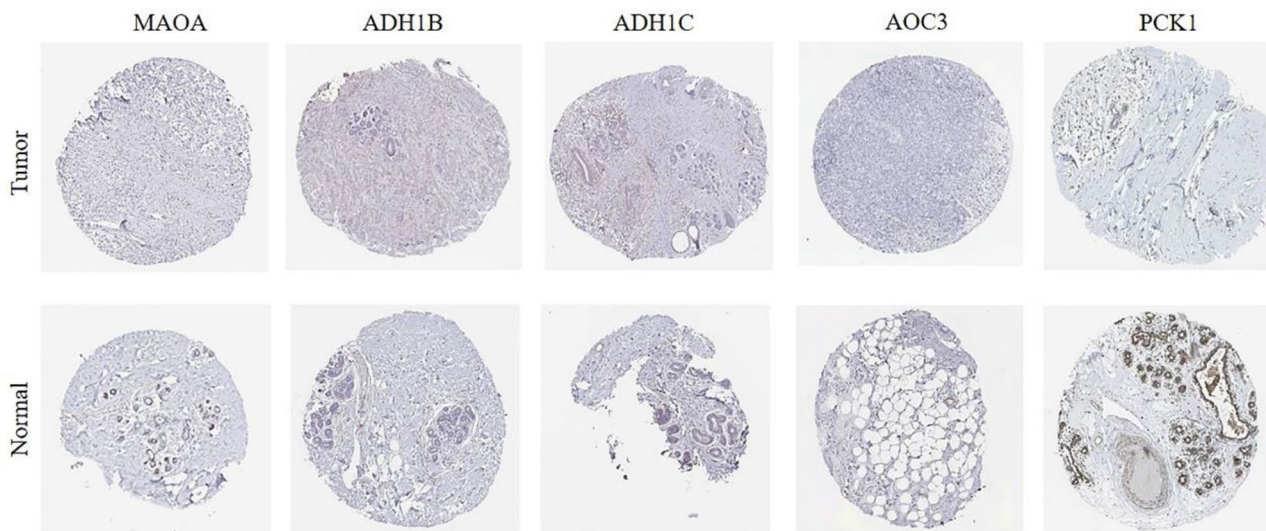
Fig. 9 The representative immunohistochemistry (IHC) images of MAOA, ADH1B, ADH1C, AOC3, and PCK1 in BC and normal tissues were extracted from the HPA database. In each set, tumor tissue sections were displayed on the upper side, and normal tissue sections were displayed on the lower side
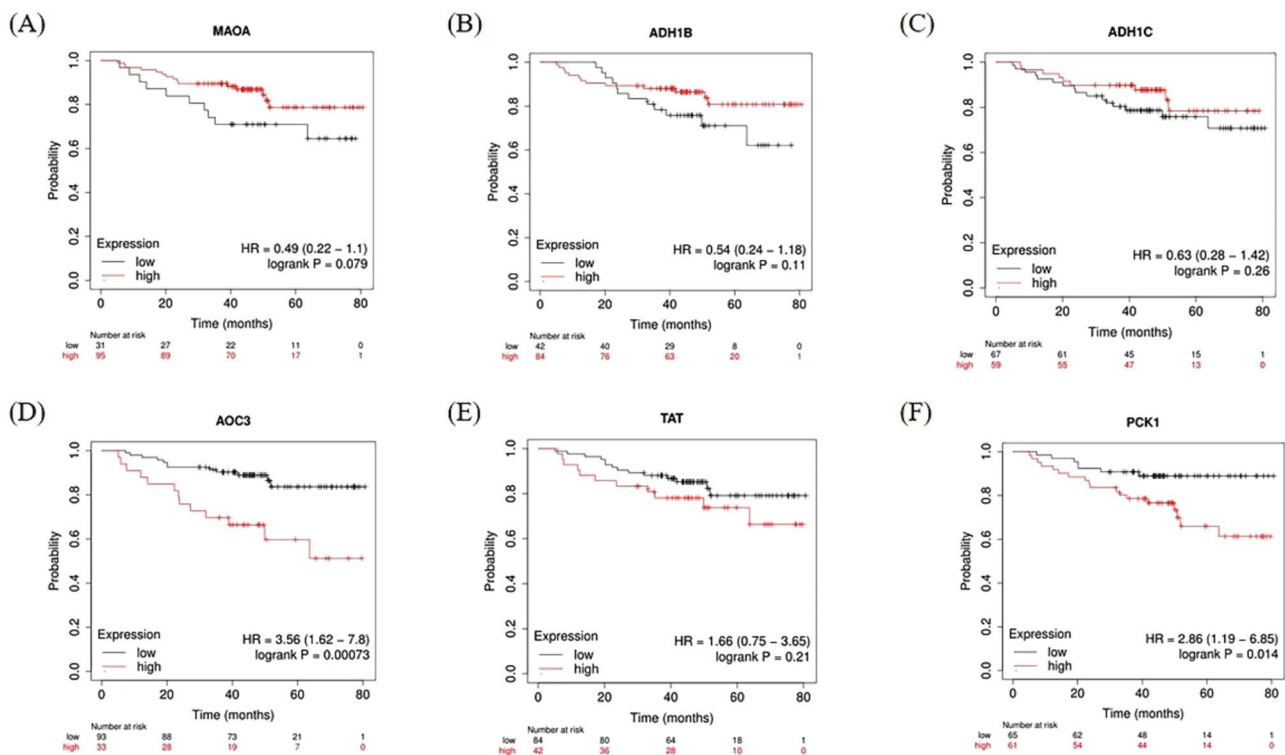
Fig. 10 Overall survival (OS) data evaluating the prognostic value of (**A**)MAOA, (**B**)ADH1B, (**C**)ADH1C, (**D**)AOC3, (**E**)TAT, and (**F**)PCK1 in TNBC patients using Kaplan-Meier plotter

the interactions between selected metabolites and genes within dysregulated pathways.

The current study employed an untargeted metabolomics approach, utilizing ultra-high-performance liquid chromatography coupled with mass spectrometry (UHPLC-MS) and multivariate statistical analysis to identify metabolites with altered levels in TNBC compared to HC. This comprehensive metabolomic analysis identified 13 upregulated metabolites and 9 downregulated metabolites in TNBC. Notably, among these metabolites, 7-methylguanine emerged as a potential biomarker for TNBC, as evidenced by ROC analysis and the DeLong

Gong *et al. Journal of Translational Medicine*   (2024) 22:1016

Page 14 of 17

test. Furthermore, MSEA highlighted several disrupted metabolic pathways critical to TNBC pathophysiology, including the malate-aspartate shuttle and the TCA cycle. These pathways play essential roles in cellular energy metabolism, indicating their significant involvement in the metabolic reprogramming characteristic of TNBC.

To deepen our understanding of the underlying mechanisms of TNBC, we analyzed data combined from three distinct GEO datasets. This comprehensive analysis included 26 samples of normal breast tissue and 101 samples of TNBC tissue. From this, we identified a total of 160 DEGs, comprising 103 downregulated and 57 upregulated genes in TNBC tissues. Functional enrichment analysis of these DEGs highlighted their significant involvement in cell proliferation processes, including cell division, mitotic spindle organization, chromosome segregation, and the positive regulation of chromosome segregation, all of which are consistent with the hallmark rapid proliferation of TNBC cells. Furthermore, KEGG pathway enrichment analysis revealed that the DEGs were predominantly associated with the PPAR signaling pathway and tyrosine metabolism. This suggests that these genes play a critical role in regulating fatty acid and amino acid metabolism within TNBC cells.

The integrative analysis of metabolomic and transcriptomic datasets has significantly advanced our understanding of the interplay between metabolic dysregulation and gene expression alterations in TNBC. This analysis has highlighted key pathways, including tyrosine metabolism, phenylalanine metabolism, and glycolysis/gluconeogenesis, underscoring the complex biological landscape of TNBC that extends beyond simple genomic alterations. The disruption of these pathways likely reflects the adaptive oncogenic processes characteristic of TNBC, presenting potential targets for therapeutic intervention. Notably, the analysis identified two DMs (4-hydroxyphenylacetaldehyde and oxalacetic acid) and six DEGs (MAOA, ADH1B, ADH1C, AOC3, TAT, and PCK1) as integral components of these pathways. Further validation using the GEPIA, UALCAN, HPA databases and western blot analysis revealed consistent expression patterns for these hub genes at both the RNA and protein levels, reinforcing their pivotal role in the pathophysiology of TNBC.

The disruption of tyrosine and phenylalanine metabolism has been linked to various pathologies, including gastroesophageal malignancies [27], non-small cell lung cancer [10], and BC [28]. Research by Christofk et al. [28] demonstrated that invasive breast cancer cells, when faced with amino acid deprivation, utilize extracellular matrix internalization and lysosomal degradation to acquire amino acids. This adaptive mechanism is crucial for supporting cellular proliferation and enhancing migratory capabilities, indicating a metabolic

dependency on phenylalanine and tyrosine. In our study, we found that 4-hydroxyphenylacetaldehyde, along with the genes MAOA, AOC3, and TAT, were significantly enriched in the tyrosine and phenylalanine metabolic pathways. This finding suggests that TNBC cells may rely on these metabolic pathways to drive tumorigenesis.

Nowadays, the treatment landscape for TNBC remains challenging, with chemotherapy being the primary option available to patients. Receptor tyrosine kinases (RTKs) are, however, intriguing druggable targets due to their high expression in TNBC [8]. RTKs are membrane-bound receptors essential for cell function, mediating intercellular signal transduction by phosphorylating tyrosine residues on key intracellular substrate proteins. This activation triggers multiple intracellular signaling pathways, such as MAPK, PI3K/Akt, and JAK/STAT, which regulate processes including cell proliferation, differentiation, metabolism, and migration [29, 30]. In TNBC cells, multiple oncogenic signaling pathways are activated downstream of RTKs. Consequently, monoclonal antibodies and small molecule inhibitors [31], such as EGFR inhibitors (e.g., erlotinib and gefitinib), VEGFR inhibitors (e.g., bevacizumab), c-MET inhibitors (e.g., cabozantinib), and FGFR inhibitors (e.g., erdafitinib), are being investigated as potential treatment options for TNBC. Tyrosine metabolism is closely linked to the activation of tyrosine kinases, indicating that alterations in this metabolic pathway can significantly influence kinase activity. Our study suggested that MAOA, AOC3, and TAT may serve as therapeutic targets for the future treatment of TNBC.

The MAOA gene encodes the enzyme monoamine oxidase-A, which is present in both peripheral tissues and the central nervous system and is essential for breaking down monoamines such as norepinephrine (NE), epinephrine, and dopamine [32]. Recent findings have shown that different cancer types exhibit unique patterns of MAOA regulation and functionality. Overexpression of MAOA has been observed in glioma [33], classical Hodgkin lymphomas [34], and prostate cancer [35]. In contrast, a trend toward decreased MAOA expression has been reported in pancreatic ductal adenocarcinoma [36], hepatocellular carcinoma (HCC) [32], and gastric cancer [37]. Notably, prior researches have consistently demonstrated a significant reduction in MAOA expression in invasive BC compared to noncancerous cells and normal breast tissue [38, 39], corroborating the findings of our study. A recent report by Wang et al. [6] highlighted the role of NE, derived from tyrosine, in modulating inflammatory immune responses within the tumor microenvironment through interactions with beta-adrenergic receptors (β-ARs), thereby influencing tumor cell invasion and migration. Suppressing the effects of the NK cell-enriched environment and diminishing the

Gong *et al. Journal of Translational Medicine*   (2024) 22:1016

Page 15 of 17

antitumor response can be achieved through chemical sympathectomy or β-AR pathway inhibition [10]. Additionally, it has been shown that MAOA may affect cancer development and progression by depleting neurotransmitters downstream, specifically NE, in pancreatic and liver cancers. Our study reveals MAOA's involvement in tyrosine and phenylalanine metabolism, suggesting a disruption in amino acid metabolism in TNBC patients. Moreover, a decrease in MAOA expression was observed in the TNBC cohort relative to the control group at both the mRNA and protein levels. This leads us to hypothesize that TNBC may exhibit elevated NE levels, potentially activating immune cells for antitumor responses—a hypothesis that warrants further investigation.

The AOC3 gene encodes the enzyme amine oxidase copper-containing 3, a membrane-bound adhesion protein also known as vascular adhesion protein 1 (VAP-1) [40]. This multifunctional molecule, primarily located in the vascular endothelium and pericytes, plays a crucial role in facilitating leukocyte adhesion and trafficking to inflammatory tissues [41]. Research suggests that VAP-1 contributes to the recruitment of tumor-infiltrating lymphocytes to various carcinomas, aiding in the destruction of cancer cells [42]. However, AOC3 has also been implicated in the progression of cancers such as melanoma and lymphoma [43]. Paradoxically, its expression is decreased in certain aggressive cancer types, including prostate and colorectal cancers [42, 43]. Our results indicated a significant reduction in AOC3 expression in TNBC, suggesting that this decrease may be associated with increased tumor aggressiveness. Moreover, our research has shown a correlation between low AOC3 expression and poor prognostic outcomes in TNBC, highlighting its potential as a prognostic biomarker. This proposition is further supported by proteomic analyses from Shaheed et al., [44] which compared neoplastic breast tissue to benign counterparts and found a significant reduction in AOC3 expression, reinforcing its prognostic relevance in breast cancer.

The precise mechanisms underlying the relationship between low AOC3 expression and poor prognostic outcomes remain unclear. However, one potential mechanism involves its role in tumor immunity. AOC3 facilitates lymphocyte adhesion to endothelial cells, promoting lymphocyte aggregation within tumor vasculature. This aggregation triggers a local immune response by activating tumor-infiltrating lymphocytes, which may inhibit tumor growth [45]. The absence or reduction of AOC3 expression in TNBC could, therefore, diminish local immune responses, contributing to a worse prognosis. Further research is needed to elucidate and validate this hypothesized link.

The TAT gene is essential for the biosynthesis of tyrosine aminotransferase, a liver-specific mitochondrial enzyme crucial for converting tyrosine into non-toxic molecules. These molecules are then either excreted via the renal pathway or used in metabolic processes to generate energy. Mutations in the TAT gene can lead to enzyme deficiency, resulting in the harmful accumulation of tyrosine and its derivatives [46]. This buildup can damage vital organs such as the liver, kidneys, and nervous system, as well as other tissues, by disrupting their normal functions. Reduced TAT expression has been observed in HCC, suggesting its involvement in the pathogenesis of this malignancy. Further in vitro analyses have shown that TAT is instrumental in mediating apoptotic pathways and exerting anti-oncogenic effects, highlighting a significant association with the development and progression of HCC [46]. Our study revealed a marked decrease in TAT protein levels and an increase in 4-hydroxyphenylacetaldehyde, a tyrosine metabolite, in patients with TNBC compared to the control group. This finding not only indicates a disruption in tyrosine metabolism within TNBC but also suggests that the downregulation of TAT may contribute to TNBC progression.

Cancer cells are characterized by significant reprogramming of cellular energy metabolism, a phenomenon predominantly illustrated by the Warburg effect [22]. This effect, observed even in oxygen-rich environments, is marked by a substantial increase in glucose uptake, enhanced glycolysis, and increased production of lactic acid within tumor cells [47, 48]. Concurrently, gluconeogenesis—the synthesis of glucose from non-carbohydrate sources such as glucogenic amino acids, pyruvate, lactate, and glycerol—is typically suppressed due to the preferential activation of the glycolysis pathway in cancer cells [49]. In our investigation, we observed an enrichment of oxaloacetic acid and PCK1 during the metabolic processes of glycolysis and gluconeogenesis. This observation suggested a critical involvement of these components in facilitating the interconnected pathways of energy metabolism within cancer cells, highlighting their potential roles in the metabolic reprogramming associated with oncogenesis.

The PCK1 gene, localized on the chromosomal region 20q13.31 in humans, exhibits variable expression across different tumor types, showing overexpression in colorectal and melanoma malignancies, while underexpression is observed in HCC and renal cell carcinoma [50, 51]. Research by Bian et al. [51] demonstrated that enhancing the stability of the PCK1-encoded protein can increase gluconeogenesis, decrease glycolysis, and suppress cancer cell proliferation. As a pivotal enzyme in gluconeogenesis, PCK1 catalyzes the conversion of oxaloacetic acid into phosphoenolpyruvate. Our findings indicate a notable increase in oxaloacetate levels, accompanied by reduced PCK1 expression in TNBC patients, suggesting an inhibition of gluconeogenesis. Additionally, our study

Gong *et al. Journal of Translational Medicine*   (2024) 22:1016

Page 16 of 17

identified a significant association between PCK1 overexpression and decreased OS in TNBC patients ($p<0.05$), aligning with previous research outcomes [47].

Our findings represented a groundbreaking contribution towards identifying potential biomarkers for TNBC. Nevertheless, these promising findings are tempered by certain limitations inherent in our study, such as the relatively small sample size, and the imperative for subsequent validation across larger and more varied cohorts. Moreover, the analytic procedures employed necessitate rigorous replication and standardization before their integration into clinical application.

In conclusion, our research underlined the utility of combining metabolomic and transcriptomic analyses to provide a more comprehensive view of the complexities of TNBC. It unveils potential diagnostic biomarkers and therapeutic targets, offering promising avenues for revolutionizing TNBC management. The imperative for future investigations to validate these findings and extend the omics-based methodology to additional cancer subtypes is clear. Such endeavors are crucial for propelling the field of personalized medicine forward in the realm of oncology, potentially enhancing patient outcomes through more tailored and effective treatment strategies.

Supplementary Information

The online version contains supplementary material available at https://doi.org/10.1186/s12967-024-05843-y.

Supplementary Material 1

Supplementary Material 2

Author contributions
Study concept and design: CF and ZL. Acquisition of data: SG, RH, MW, and FL. Analysis and interpretation of data: SG and QW. Drafting of the manuscript: SG and ZL. Critical revision of the manuscript for important intellectual content: all the authors.

Data availability
Not applicable.

Declarations

Ethics approval and consent to participate
The study was conducted under the Declaration of Helsinki and approved by the Ethics Committee of the Second Affiliated Hospital of Fujian Medical University (Approval number: 2021[168]). Written informed consent was obtained from individual or guardian participants.

Consent for publication
Not applicable.

Competing interests
The authors declare no competing financial interests.

References

1. Ma J, Chen C, Liu S, Ji J, Wu D, Huang P, et al. Identification of a five genes prognosis signature for triple-negative breast cancer using multi-omics methods and bioinformatics analysis. Cancer Gene Ther. 2022;29(11):1578–89. https://doi.org/10.1038/s41417-022-00473-2.
2. Yuan Q, Zheng L, Liao Y, Wu G. Overexpression of CCNE1 confers a poorer prognosis in triple-negative breast cancer identified by bioinformatic analysis. World J Surg Oncol. 2021;19(1). https://doi.org/10.1186/s12957-021-02200-x.
3. Bissanum R, Kamolphiwong R, Navakanitworakul R, Kanokwiroon K. Integrated bioinformatic analysis of potential biomarkers of poor prognosis in triple-negative breast cancer. Translational Cancer Res. 2022;11(9):3039–49. https://doi.org/10.21037/tcr-22-662.
4. Lin X, He S, Wu S, Zhang T, Gong S, Minjie T, et al. Diagnostic biomarker panels of osteoarthritis: UPLC-QToF/MS-based serum metabolic profiling. Peerj. 2023;11. https://doi.org/10.7717/peerj.14563.
5. Li L, Zheng X, Zhou Q, Villanueva N, Nian W, Liu X, et al. Metabolomics-based Discovery of Molecular signatures for Triple negative breast Cancer in Asian Female Population. Sci Rep. 2020;10(1):370. https://doi.org/10.1038/s41598-019-57068-5. Epub 2020/01/17.
6. Yamashita Y, Nishiumi S, Kono S, Takao S, Azuma T, Yoshida M. Differences in elongation of very long chain fatty acids and fatty acid metabolism between triple-negative and hormone receptor-positive breast cancer. BMC Cancer. 2017;17(1):589. https://doi.org/10.1186/s12885-017-3554-4. Epub 2017/08/31.
7. Beatty A, Fink LS, Singh T, Strigun A, Peter E, Ferrer CM, et al. Metabolite Profiling reveals the Glutathione Biosynthetic Pathway as a therapeutic target in Triple-negative breast Cancer. Mol Cancer Ther. 2018;17(1):264–75. https://doi.org/10.1158/1535-7163.MCT-17-0407. Epub 2017/10/13.
8. Lanning NJ, Castle JP, Singh SJ, Leon AN, Tovar EA, Sanghera A, et al. Metabolic profiling of triple-negative breast cancer cells reveals metabolic vulnerabilities. Cancer Metabolism. 2017;5(1):6.
9. Resurreccion EP, Fong K-w. The integration of Metabolomics with other Omics: insights into understanding prostate Cancer. Metabolites. 2022;12(6). https://doi.org/10.3390/metabo12060488.
10. Lee H-S, Ruiying C, Zeyun L, Yongliang Y, Zijia Z, Ji Z, et al. A comprehensive analysis of metabolomics and transcriptomics in non-small cell lung cancer. PLoS ONE. 2020;15(5). https://doi.org/10.1371/journal.pone.0232272.
11. Peng Y, Yin D, Li X, Wang K, Li W, Huang Y, et al. Integration of transcriptomics and metabolomics reveals a novel gene signature guided by FN1 associated with immune response in oral squamous cell carcinoma tumorigenesis. J Cancer Res Clin Oncol. 2023;149(9):6097–113. https://doi.org/10.1007/s00432-023-04572-x.
12. Du B, Zhang F, Zhou Q, Cheng W, Yu Z, Li L, et al. Joint analysis of the metabolomics and transcriptomics uncovers the dysregulated network and develops the diagnostic model of high-risk neuroblastoma. Sci Rep. 2023;13(1). https://doi.org/10.1038/s41598-023-43988-w.
13. Smith CA, Want EJ, O'Maille G, Abagyan R, Siuzdak G. XCMS: processing mass spectrometry data for metabolite profiling using nonlinear peak alignment, matching, and identification. Anal Chem. 2006;78(3):779–87. Epub 2006/02/02. https://doi.org/10.1021/ac051437y. PubMed PMID: 16448051.
14. Zhang M, Chen H, Wang M, Bai F, Wu K. Bioinformatics analysis of prognostic significance of COL10A1 in breast cancer. Biosci Rep. 2020;40(2). https://doi.org/10.1042/bsr20193286.
15. Chandrashekar D, Bashel B, Balasubramanya S, Creighton C, Ponce-Rodriguez I, Chakravarthi B, et al. UALCAN: a portal for facilitating Tumor Subgroup Gene expression and survival analyses. Neoplasia. 2017;19(8):649–58. https://doi.org/10.1016/j.neo.2017.05.002. PubMed PMID: 28732212.
16. Ying B, Xu W, Nie Y, Li Y. HSPA8 is a New Biomarker of Triple negative breast Cancer related to prognosis and Immune Infiltration. Dis Markers. 2022. https://doi.org/10.1155/2022/8446857. 2022:8446857. Epub 2022/12/02.

17. Gong S, Wang Q, Huang J, Huang R, Chen S, Cheng X, et al. LC-MS/MS platform-based serum untargeted screening reveals the diagnostic biomarker panel and molecular mechanism of breast cancer. Methods. 2024;222:100–11. PubMed PMID: 38228196.

18. Nie Y, Huang F, Lou L, Yan J. The obesity-related metabolic gene HSD17B8 protects against breast Cancer: high RNA/Protein expression means a better prognosis. Med Sci Monit. 2021;28. https://doi.org/10.12659/msm.934424.

19. Gong Y, Ji P, Yang YS, Xie S, Yu TJ, Xiao Y, et al. Metabolic-pathway-based subtyping of Triple-negative breast Cancer reveals potential therapeutic targets. Cell Metab. 2021;33(1):51–64. https://doi.org/10.1016/j.cmet.2020.10.012. e9. Epub 2020/11/13.

20. Sai Baba KSS, Rehman MA, Pradeep Kumar J, Fatima M, Raju GSN, Uppin SG, et al. Serum human epididymis Protein-4 (HE4) - a novel Approach to differentiate malignant Frombenign breast tumors. Asian Pac J Cancer Prev. 2021;22(8):2509–7. PubMed PMID: 34452565; PubMed Central PMCID: PMCPMC8629466.

21. Martinez-Outschoorn U, Peiris-Pagés M, Pestell R, Sotgia F, Lisanti MJNC. Cancer metabolism: a therapeutic perspective. Nat Rev Clin Oncol. 2017;14(1):11–31. https://doi.org/10.1038/nrclinonc.2016.60. PubMed PMID: 27141887.

22. Li Z, Sun C, Qin Z. Metabolic reprogramming of cancer-associated fibroblasts and its effect on cancer cell reprogramming. Theranostics. 2021;11(17):8322–36. https://doi.org/10.7150/thno.62378.

23. Li J, Liu K, Ji Z, Wang Y, Yin T, Long T, et al. Serum untargeted metabolomics reveal metabolic alteration of non-small cell lung cancer and refine disease detection. Cancer Sci. 2023;114(2):680–9. https://doi.org/10.1111/cas.15629. PubMed PMID: 36310111.

24. Nunes S, Sousa J, Silva F, Silveira M, Guimarães A, Serpa J, et al. Peripheral blood serum NMR metabolomics is a powerful Tool to discriminate benign and malignant ovarian tumors. Metabolites. 2023;13(9). https://doi.org/10.3390/metabo13090989. PubMed PMID: 37755269.

25. Wu S, Xue W, Yu H, Yu H, Shi Z, Wang L, et al. Serum uric acid levels and health outcomes in CKD: a prospective cohort study. Nephrol Dial Transpl. 2023. https://doi.org/10.1093/ndt/gfad201. PubMed PMID: 37698875.

26. Zhang X, Kang X, Jin L, Bai J, Zhang H, Liu W, et al. ABCC9, NKAPL, and TMEM132C are potential diagnostic and prognostic markers in triple-negative breast cancer. Cell Biol Int. 2020;44(10):2002–10. https://doi.org/10.1002/cbin.11406.

27. Wiggins T, Kumar S, Markar SR, Antonowicz S, Hanna GB. Tyrosine, phenylalanine, and Tryptophan in gastroesophageal malignancy: a systematic review. Cancer Epidemiol Biomarkers Prev. 2015;24(1):32–8. https://doi.org/10.1158/1055-9965.Epi-14-0980.

28. Christofk H, Nazemi M, Yanes B, Martinez ML, Walker HJ, Pham K, et al. The extracellular matrix supports breast cancer cell growth under amino acid starvation by promoting tyrosine catabolism. PLoS Biol. 2024;22(1). https://doi.org/10.1371/journal.pbio.3002406.

29. Sudhesh Dev S, Zainal Abidin SA, Farghadani R, Othman I, Naidu R. Receptor tyrosine kinases and their signaling pathways as therapeutic targets of Curcumin in Cancer. Front Pharmacol. 2021;12. https://doi.org/10.3389/fphar.2021.772510.

30. Duan L, Calhoun S, Perez RE, Macias V, Mir F, Pergande MR, et al. Prolyl Carboxypeptidase Maintains Receptor Tyrosine Kinase Signaling and is a potential therapeutic target in Triple negative breast Cancer. Cancers. 2022;14(3). https://doi.org/10.3390/cancers14030739.

31. Mehlich D, Marusiak AA. Kinase inhibitors for precision therapy of triple-negative breast cancer: Progress, challenges, and new perspectives on targeting this heterogeneous disease. Cancer Lett. 2022;547. https://doi.org/10.1016/j.canlet.2022.215775.

32. Pang YY, Li JD, Gao L, Yang X, Dang YW, Lai ZF, et al. The clinical value and potential molecular mechanism of the downregulation of MAOA in hepatocellular carcinoma tissues. Cancer Med. 2020;9(21):8004–19. https://doi.org/10.1002/cam4.3434.

33. Kushal S, Wang W, Vaikari VP, Kota R, Chen K, Yeh TS, et al. Monoamine oxidase A (MAO A) inhibitors decrease glioma progression. Oncotarget. 2016;7(12):13842–53.

34. Li P, Siddiqi I, Mottok A, Loo E, Wu C, Cozen W, et al. Monoamine oxidase A is highly expressed in classical Hodgkin lymphoma. J Pathol. 2017;243(2):220–9. https://doi.org/10.1002/path.4944. PubMed PMID: 28722111.

35. Gaur S, Gross M, Liao C, Qian B, Shih JJTP. Effect of Monoamine oxidase A (MAOA) inhibitors on androgen-sensitive and castration-resistant prostate cancer cells. Prostate. 2019; 79(6):667–77. https://doi.org/10.1002/pros.23774. PubMed PMID: 30693539.

36. Oria VO, Bronsert P, Thomsen AR, Föll MC, Zamboglou C, Hannibal L, et al. Proteome Profiling of primary pancreatic ductal adenocarcinomas undergoing additive chemoradiation link ALDH1A1 to early local recurrence and Chemoradiation Resistance. Transl Oncol. 2018;11(6):1307–22. https://doi.org/10.1016/j.tranon.2018.08.001.

37. Wang Y, Wang S, Yang Q, Li J, Yu F, Zhao E, et al. Norepinephrine enhances aerobic glycolysis and May Act as a predictive factor for Immunotherapy in Gastric Cancer. J Immunol Res. 2021;2021:1–13. https://doi.org/10.1155/2021/5580672.

38. Ren Y, Jiang H, Ma D, Nakaso K, Feng JJH. Parkin degrades estrogen-related receptors to limit the expression of monoamine oxidases. Hum Mol Genet. 2011;20(6):1074–83. https://doi.org/10.1093/hmg/ddq550. PubMed PMID: 21177257.

39. Daniel A, Gaviglio A, Knutson T, Ostrander J, D'Assoro A, Ravindranathan P, et al. Progesterone receptor-B enhances estrogen responsiveness of breast cancer cells via scaffolding PELP1- and estrogen receptor-containing transcription complexes. Oncogene. 2015;34(4):506–15. https://doi.org/10.1038/onc.2013.579. PubMed PMID: 24469035.

40. Chang S-J, Tu H-P, Lai Y-CC, Luo C-W, Nejo T, Tanaka S, et al. Increased vascular adhesion protein 1 (VAP-1) levels are Associated with Alternative M2 macrophage activation and poor prognosis for human gliomas. Diagnostics. 2020;10(5). https://doi.org/10.3390/diagnostics10050256.

41. Salmi M, Jalkanen SJA. signaling r. Vascular Adhesion Protein-1: A Cell Surface Amine Oxidase in Translation. Antioxid Redox Signal. 2019;30(3):314–32. https://doi.org/10.1089/ars.2017.7418. PubMed PMID: 29065711.

42. Chen J, Xi J, Tian Y, Bova GS, Zhang H. Identification, prioritization, and evaluation of glycoproteins for aggressive prostate cancer using quantitative glycoproteomics and antibody-based assays on tissue specimens. Proteomics. 2013;13(15):2268–77. https://doi.org/10.1002/pmic.201200541.

43. Ward ST, Weston CJ, Shepherd EL, Hejmadi R, Ismail T, Adams DH. Evaluation of serum and tissue levels of VAP-1 in colorectal cancer. BMC Cancer. 2016;16(1). https://doi.org/10.1186/s12885-016-2183-7.

44. Shaheed S, Rustogi N, Scally A, Wilson J, Thygesen H, Loizidou M, et al. Identification of stage-specific breast markers using quantitative proteomics. J Proteome Res. 2013;12(12):5696–708. https://doi.org/10.1021/pr400662k. PubMed PMID: 24106833.

45. Sun W, Choi J, Cha Y, Koo J. Evaluation of the expression of Amine oxidase proteins in breast Cancer. Int J Mol Sci. 2017;18(12). https://doi.org/10.3390/ijms18122775.

46. Fu L, Dong S-S, Xie Y-W, Tai L-S, Chen L, Kong KL, et al. Down-regulation of tyrosine aminotransferase at a frequently deleted region 16q22 contributes to the pathogenesis of hepatocellular carcinoma. Hepatology. 2010;51(5):1624–34. https://doi.org/10.1002/hep.23540.

47. Alshehri B. Prognostic significance and expression pattern of glucose related genes in breast cancer: a comprehensive computational biology approach. Saudi J Biol Sci. 2024;31(1). https://doi.org/10.1016/j.sjbs.2023.103896.

48. Shah M, Shrivastava V, Sofi S, Jamous Y, Khan M, Alkholifi F, et al. Chlorogenic acid restores ovarian functions in mice with Letrozole-Induced Polycystic Ovarian Syndrome Via Modulation of Adiponectin receptor. Biomedicines. 2023;11(3). https://doi.org/10.3390/biomedicines11030900. PubMed PMID: 36979879.

49. Yustisia I, Amriani R, Cangara H, Syahrijuita S, Alfian Zainuddin A, Natsir R. High expression of FBP1 and LDHB in fibroadenomas and invasive breast cancers. Breast Dis. 2021;40(4):251–6. https://doi.org/10.3233/bd-201035.

50. Wang Z, Dong C. Gluconeogenesis in Cancer: function and regulation of PEPCK, FBPase, and G6Pase. Trends Cancer. 2019;5(1):30–45. https://doi.org/10.1016/j.trecan.2018.11.003.

51. Bian X-l, Chen H-z, Yang P-b, Li Y-p, Zhang F-n, Zhang J-y, et al. Nur77 suppresses hepatocellular carcinoma via switching glucose metabolism toward gluconeogenesis through attenuating phosphoenolpyruvate carboxykinase sumoylation. Nat Commun. 2017;8(1). https://doi.org/10.1038/ncomms14420.

Publisher's note